International Journal of
Advanced Thermofluid Research

ISSN 2455-1368
www.ijatr.org

IREEE

Finite Difference Simulation of MHD Radiative Flow of a Nanofluid past a Stretching Sheet with Stability Analysis

M. Shakhaoath Khan [1], M. Mahmud Alam [1], E. E. Tzirtzilakis [2], M. Ferdows [3]* and Ifsana Karim [1]

[1]*Mathematics Discipline; Science, Engineering and Technology School, Khulna University, Khulna-9208, Bangladesh.*
[2]*Fluid Dynamics &Turbomachinery Laboratory, Department of Mechanical Engineering, Technological Educational Institute of Western Greece, 1 M. AleksandrouStr, Koukouli, 263 34 Patras Greece.*
[3]*Research Group of Fluid Flow Modeling and Simulation, Department of Applied Mathematics, University of Dhaka, Dhaka-1000, Bangladesh.*

Keywords
Nanofluid •
Magnetic Field •
Thermal Radiation •
EFDM •
Stability Analysis.

Received
April 15, 2016
Revised
May 30, 2016
Accepted
May 12, 2016
Published
June 1, 2016

Abstract

In the present study, unsteady heat and mass nanofluid flow past a stretching sheet with the effect of thermal radiation and magnetic field was carried out. To obtain non-similar equation, the boundary layer governing equations including continuity, momentum, energy and concentration balance were non-dimensionalized by usual transformation. The non-similar approach was employed, which depends on the dimensionless parameters such as Magnetic parameter (M), Radiation parameter (R), Prandtl number (P_r), Eckert number (E_c) Lewis number (L_e), Brownian motion parameter (N_b), Thermophoresis parameter (N_t), Local Reynolds number (R_e) and velocity parameter (b/a). The temperature and concentration distributions are found affected by these dimensionless parameters. The obtained equations have been solved by explicit finite difference method (EFDM). A theoretical model of the stability and convergence to describe the aspects of the finite difference scheme was developed in this study. This analysis makes the EFDM approach more accurate and able to provide the convergence criteria of the method ($P_r \geq 0.375$ and $L_e \geq 0.25$). The temperature and concentration profiles are discussed for the different values of the dimensionless parameters by considering different time steps. The present computational investigation finds applications in the area of magnetic nanomaterials processing.

***Corresponding email**: ferdows@du.ac.bd (M. Ferdows).

DOI: https://doi.org/10.51141/IJATR.2016.2.1.3

Nomenclature

a, b	Linear stretching constants, s^{-1}
A_1, A_2	Constants depends on the properties of the fluid

B_0	Magnetic induction, Wb m^{-2}
C	Nanoparticle concentration
C_w	Nanoparticle concentration at stretching surface
C_∞	Ambient nanoparticle concentration as y tends to infinity
$\bar{C}$	Dimensionless concentration
c_p	Specific heat capacity, J kg^{-1} K^{-1}
D_B	Brownian diffusion coefficient
D_T	Thermophoresis diffusion coefficient
k	Thermal conductivity, Wm^{-1} K^{-1}
κ	Boltzmann constant, 1.3805×10^{-23} J K^{-1}
κ^*	Mean absorption coefficient
l	Characteristics length, m
P	Fluid pressure, Pa
q_r	Radiative heat flux in the y-direction, kg m^{-2}
T	Fluid temperature, K
T_w	Temperature at the stretching surface, K
T_∞	Ambient temperature as y tends to infinity, K
$\bar{T}$	Dimensionless temperature
u_w	Stretching velocity, ms^{-1}
$U_\circ$	Uniform velocity, ms^{-1}
u, v	Velocity components along x and y axes respectively, m s^{-1}
U, V	Dimensionless velocity components
x, y	Cartesian coordinates measured along stretching surface, m

Greek Symbols

υ	Kinematic viscosity of the fluid, m^2 s^{-1}
μ	Dynamic viscosity of the fluid, Pa-s
$(\rho c)_p$	Effective heat capacity of the nanoparticle, J m^{-3}K^{-1}
$(\rho c)_f$	Heat capacity of the fluid, J m^{-3}K^{-1}
α	Thermal diffusivity, m^2 s^{-1}
σ_s	Stefan-Boltzmann constant, 5.6697×10^{-8} kg m^{-2} K^{-4}
σ	Conductivity of the material, S m^{-1}
ρ_P	Nanoparticle mass density, kg m^{-3}
ρ_f	Fluid density, kg m^{-3}
τ	Dimensionless time

1. Introduction

The effects of thermal radiation on Magnetohydrodynamics (MHD) boundary layer flow have become important in several industrial, scientific and engineering fields. Due to sundry applications of MHD in heat exchangers, pumps, space vehicle propulsion, thermal protection, and in controlling fusion and the rate of cooling, etc., the flow due to a stretching surface has become more important. This study finds application in industries such as melt spinning, extrusion, glass fiber production, hot rolling, wire drawing, manufacture of plastic and rubber sheets, polymer sheet and filaments, etc. It is also employed for copper, brass, bronze and aluminum and increasingly with cast iron and steel.

Wang (1984) investigated the problem of three dimensional (3D) fluid flows due to a stretching flat plate. Na and Pop (1996) studied an unsteady flow past a stretching sheet. In the case of unsteady boundary layer flow, Sattar and Alam (1994) presented unsteady free convection and mass transfer flow of a viscous, incompressible and electrically conducting fluid past a moving infinite vertical porous plate with thermal diffusion effect. The radiative heat transfer with the viscous dissipation effect in the presence of transverse magnetic field was analyzed by Kumar (2009). Singh et al. (2010) studied the effect of thermal radiation and magnetic field on unsteady stretching permeable sheet in presence of free stream velocity. The technologies due to nanoparticles have been used over a large area. Choi (1995) was the first researcher who studied nanoparticles. The convective instability and heat transfer characteristics of the nanofluids were analyzed by Kang and Choi (2004). Jang and Choi (2007) obtained nanofluids' thermal conductivity and the various parameters affecting it. The natural Convective Boundary layer flows of a nanofluid past a vertical plate have been described by Kuznestov and Neild (2009 & 2010). In this model Brownian motion and Thermophoresis were accounted with the simplest possible boundary conditions. They also studied Cheng–Minkowycz problem for natural convective boundary-layer flow in a porous medium saturated by a nanofluid. Bachok et al. (2010) studied the steady boundary layer flow of a nanofluid past a moving semi-infinite flat plate in a uniform free stream. It was assumed that the plate was moving in the same or opposite direction to the free stream to define the resulting system of nonlinear ordinary differential equations. Recently Khan and Pop (2010 & 2011) formulated the problems of laminar boundary layer flow of a nanofluid past a stretching sheet, and free convection boundary layer nanofluid flow past a horizontal flat plate. Anjali and Andrews (2011) presented the problem of incompressible, viscous, force convective laminar boundary layer flow of copper water and alumina water nanofluids over a flat plate. The efficiency of heat transfer in nanofluids was focused in their study. MHD natural convection nanofluid flow over a linearly stretching sheet was analyzed by Hamad (2011) who presented an analytical solution technique. Hamad and Pop (2011) discussed the boundary layer flow near the stagnation-point flow on a permeable stretching sheet in a porous medium saturated with a nanofluid. Hamad et al. (2011) investigated free convection flow of a nanofluid past a semi-infinite vertical flat plate with the influence of magnetic field. Ferdows and Hamad (2012) studied a similarity solution of boundary layer stagnation-point of nanofluid flow, and also investigated viscous flow with heat transfer of nanofluid over nonlinearly stretching sheet. Takabi et al. (2014 & 2015) have investigated heat and fluid flow in nanofluids by adopting single-phase model which was found accurate enough to capture the thermal and hydrodynamic effects of a nanofluid flow.

In recent years, many studies have been reported on mathematical modeling and simulations of boundary layer heat and mass nanofluid flow (Ferdows et al., 2012 & 2014; Khan et al., 2012, 2013 & 2014; Beg et al., 2014; Wahiduzzamanet al., 2015a&b). However, the aim of the present study is unsteady boundary layer nanofluid flow over a stretching surface with the influence of magnetic and thermal radiation effect. The explicit finite difference method (EFDM) (Carnahan et al., 1969) has been used with stability and convergence analysis to solve the obtained non- similar equations.

The application of the present study is the manufacturing of Magnetic nanofluids and electro-conductive nanofluid suspensions (Beg et al., 2014).

2. Mathematical Model of the Flow

The physical configuration and coordinate system are shown in Figure 1. Considering the Cartesian coordinates, x is measured along the stretching surface and y is normal to the stretching surface.

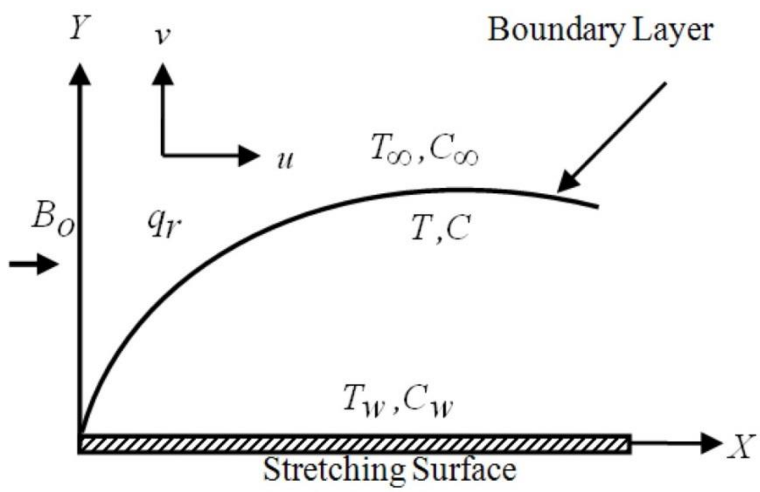

Figure 1. Physical model and coordinate system.

The flow takes place at $y \geq 0$. An unsteady uniform stress leading to equal and opposite forces is applied along the x-axis so that the sheet is stretched keeping the origin fixed. Initially it is assumed that fluid and the plate are at rest after that the plate is moved with a constant velocity U_0 in its own plane. Instantaneously at time $t > 0$, the temperature of the plate and species concentration are raised to $T_w\left(>T_\infty\right)$ and $C_w\left(>C_\infty\right)$ respectively, which are thereafter maintained constant, where T_w, C_w are temperature and species concentration at the wall and T_∞, C_∞ are temperature and species concentration far away from the plate, respectively. A uniform magnetic field B_0 is imposed to the plate. The magnetic induction vector B_0 can be taken as $B = (0, B_0, 0)$ and q_r is radiative heat flux in the y-direction. Under the usual boundary layer approximation, the MHD unsteady nanofluid flow and heat and mass transfer with the radiation effect are governed by the following equations:

The Continuity equation:

$$\frac{\partial u}{\partial x}+\frac{\partial v}{\partial y}=0 \tag{1}$$

The Momentum equation:

$$\frac{\partial u}{\partial t}+u\frac{\partial u}{\partial x}+v\frac{\partial u}{\partial y}=U_\circ\frac{dU}{dx}+\upsilon\frac{\partial^2 u}{\partial y^2}+\frac{\sigma B_0{}^2}{\rho}(U_\circ-u) \tag{2}$$

The Energy equation:

$$\frac{\partial T}{\partial t}+u\frac{\partial T}{\partial x}+v\frac{\partial T}{\partial y}=\alpha\frac{\partial^2 T}{\partial y^2}-\frac{\alpha}{k}\frac{\partial q_r}{\partial y}+\frac{\upsilon}{c_p}\left(\frac{\partial u}{\partial y}\right)^2+\tau\left\{D_B\left(\frac{\partial T}{\partial y}\cdot\frac{\partial C}{\partial y}\right)+\frac{D_T}{T_\infty}\left(\frac{\partial T}{\partial y}\right)^2\right\} \quad (3)$$

The Concentration equation:

$$\frac{\partial C}{\partial t}+u\frac{\partial C}{\partial x}+v\frac{\partial C}{\partial y}=D_B\frac{\partial^2 C}{\partial y^2}+\frac{D_T}{T_\infty}\frac{\partial^2 T}{\partial y^2}. \quad (4)$$

The initial and boundary conditions are:

$$\begin{aligned} &t=0,\, u_w=U_0=ax,\, v=0, T=T_\infty,\, C=C_\infty, \text{ everywhere}\\ &t\geq 0,\, u=0,\, v=0,\, T=T_\infty,\, C=C_\infty \quad \text{at } x=0\\ &u=U=bx,\; v=0,\; T=T_w,\; C=C_w \quad \text{at } y=0\\ &u=0,\, v=0,\, T\to T_\infty,\, C\to C_\infty \quad \text{as } y\to\infty \end{aligned} \quad (5)$$

where α is the thermal diffusivity, k is the thermal conductivity, D_B is the Brownian diffusion coefficient, D_T is the thermophoresis diffusion coefficient, x is the coordinate measured along stretching surface, u_w is the stretching velocity and U is the uniform velocity. The Rosseland approximation (1968) is expressed for radiative heat flux and leads to the form as:

$$q_r=-\frac{4\sigma}{3\kappa^*}\frac{\partial T^4}{\partial y} \quad (6)$$

where σ is the Stefan-Boltzmann constant and κ^* is the mean absorption coefficient. The temperature difference within the flow is sufficiently small such that T^4 may be expressed as a linear function of the temperature; then the Taylor's series for T^4 about T_∞ after neglecting higher order terms:

$$T^4=4T_\infty^{\;3}-3T_\infty^{\;4}. \quad (7)$$

Introducing the following non dimensional variables:

$$X=\frac{xU_0}{\upsilon},\quad Y=\frac{yU_0}{\upsilon},\quad U=\frac{u}{U_0},\quad V=\frac{v}{U_0},$$

$$\tau=\frac{tU_0^2}{\upsilon},\quad \bar{T}=\frac{T-T_\infty}{T_w-T_\infty},\quad \bar{C}=\frac{C-C_\infty}{C_w-C_\infty},$$

Then Eqs. (1) to (5) become:

$$\frac{\partial U}{\partial X}+\frac{\partial V}{\partial Y}=0 \quad (8)$$

$$\frac{\partial U}{\partial \tau}+U\frac{\partial U}{\partial X}+V\frac{\partial U}{\partial Y}=\frac{1}{R_e}\left(\frac{b^2}{a^2}\right)+\frac{\partial^2 U}{\partial Y^2}+M(1-U) \quad (9)$$

$$\frac{\partial \bar{T}}{\partial \tau}+U\frac{\partial \bar{T}}{\partial X}+V\frac{\partial \bar{T}}{\partial Y}=\left(\frac{1+R}{P_r}\right)\frac{\partial^2 \bar{T}}{\partial Y^2}+E_c\left(\frac{\partial U}{\partial Y}\right)^2+N_b\left(\frac{\partial \bar{T}}{\partial Y}\cdot\frac{\partial \bar{C}}{\partial Y}\right)+N_t\left(\frac{\partial \bar{T}}{\partial Y}\right)^2 \quad (10)$$

$$\frac{\partial \bar{C}}{\partial \tau}+U\frac{\partial \bar{C}}{\partial X}+V\frac{\partial \bar{C}}{\partial Y}=\frac{1}{L_e}\left[\frac{\partial^2 \bar{C}}{\partial Y^2}+\left(\frac{N_t}{N_b}\right)\frac{\partial^2 \bar{T}}{\partial Y^2}\right]. \tag{11}$$

The non-dimensional boundary conditions are;

$\tau \le 0,\ U=0,\ V=0,\ \bar{T}=0,\ \bar{C}=0$, everywhere (12)

$\tau > 0,\ U=0,\ V=0,\ \bar{T}=0,\ \bar{C}=0$ at $X=0$

$U=1,\ V=0,\ \bar{T}=1,\ \bar{C}=1$ at $Y=0$ (13)

$U=0,\ V=0,\ \bar{T}=0,\ \bar{C}=0$ as $Y\to\infty$

where, $M=\dfrac{\sigma B_0^{\,2}\nu}{\rho U_0^2}$, is the Magnetic parameter, $R=\dfrac{16\sigma T_\infty^{\,3}}{3k\kappa^*}$, is the Radiation parameter,

$P_r=\dfrac{\upsilon}{\alpha}$, is the Prandtl number, $E_c=\dfrac{U_0^{\,2}}{c_p(T_w-T_\infty)}$, is the Eckert number,

$L_e=\dfrac{\upsilon}{D_B}$, is the Lewis number, $N_b=\dfrac{\tau D_B\left(C_w-C_\infty\right)}{\upsilon}$, is the Brownian parameter,

$N_t=\dfrac{D_T}{T_\infty}\dfrac{\tau}{\nu}\left(T_w-T_\infty\right)$, is the Thermophoresis parameter, $R_e=\dfrac{xu_w}{\upsilon}$, is the Local Reynolds number and

$\dfrac{b}{a}$, is the velocity parameter.

3. Numerical Technique

In order to solve the non-similar unsteady coupled non-linear partial differential equations, the explicit finite difference method has been used. Here the plate of height $X_{\max}\left(=100\right)$ is considered i.e. X varies from 0 to 100 and assumed $Y_{\max}\left(=25\right)$ as corresponding to $Y\to\infty$ i.e. Y varies from 0 to 25.

There are $m\left(=125\right)$ and $n\left(=125\right)$ grid spacing in the X and Y directions respectively as shown in Figure 2. It is assumed that ΔX, ΔY are constant mesh sizes along X and Y directions respectively and taken as follows:

$\Delta X=0.8\left(0\le X\le 100\right)$ and $\Delta Y=0.2\left(0\le Y\le 25\right)$ with the smaller time-step, $\Delta\tau=0.005$.

Let U', V', $\bar{T}'$ and $\bar{C}'$ denote the values of U, V, $\bar{T}$ and $\bar{C}$ at the end of a time-step respectively. Using the explicit finite difference approximation, the following appropriate set of finite difference equations are obtained as:

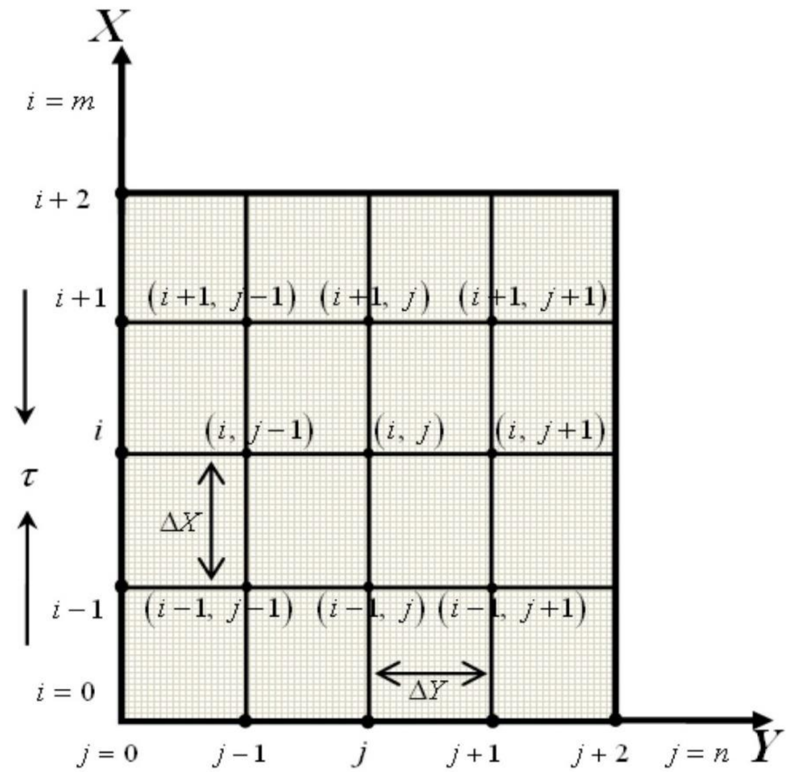

Figure 2. Finite difference space grid.

$$\frac{U'_{i,j}-U'_{i-1,j}}{\Delta X}+\frac{V_{i,j}-V_{i,j-1}}{\Delta Y}=0 \tag{14}$$

$$\frac{U'_{i,j}-U_{i,j}}{\Delta\tau}+U_{i,j}\frac{U_{i,j}-U_{i-1,j}}{\Delta X}+V_{i,j}\frac{U_{i,j+1}-U_{i,j}}{\Delta Y}=\frac{1}{R_e}\left(\frac{b^2}{a^2}\right)+\frac{U_{i,j+1}-2U_{i,j}+U_{i,j-1}}{\left(\Delta Y\right)^2}+M\left(1-U_{i,j}\right) \tag{15}$$

$$\begin{aligned}\frac{\overline{T}'_{i,j}-\overline{T}_{i,j}}{\Delta\tau}+U_{i,j}\frac{\overline{T}_{i,j}-\overline{T}_{i-1,j}}{\Delta X}+V_{i,j}\frac{\overline{T}_{i,j+1}-\overline{T}_{i,j}}{\Delta Y}&=\left(\frac{1+R}{P_r}\right)\left(\frac{\overline{T}_{i,j+1}-2\overline{T}_{i,j}+\overline{T}_{i,j-1}}{\left(\Delta Y\right)^2}\right)+E_c\left(\frac{U_{i,j+1}-U_{i,j}}{\Delta Y}\right)^2\\&+N_b\left(\frac{\overline{T}_{i,j+1}-\overline{T}_{i,j}}{\Delta Y}\cdot\frac{\overline{C}_{i,j+1}-\overline{C}_{i,j}}{\Delta Y}\right)+N_t\left(\frac{\overline{T}_{i,j+1}-\overline{T}_{i,j}}{\Delta Y}\right)^2\end{aligned} \tag{16}$$

$$\begin{aligned}&\frac{\overline{C}'_{i,j}-\overline{C}_{i,j}}{\Delta\tau}+U_{i,j}\frac{\overline{C}_{i,j}-\overline{C}_{i-1,j}}{\Delta X}+V_{i,j}\frac{\overline{C}_{i,j+1}-\overline{C}_{i,j}}{\Delta Y}\\&=\frac{1}{L_e}\left[\left(\frac{\overline{C}_{i,j+1}-2\overline{C}_{i,j}+\overline{C}_{i,j-1}}{\left(\Delta Y\right)^2}\right)+\frac{N_t}{N_b}\left(\frac{\overline{T}_{i,j+1}-2\overline{T}_{i,j}+\overline{T}_{i,j-1}}{\left(\Delta Y\right)^2}\right)\right]\end{aligned} \tag{17}$$

with initial and boundary conditions:

$$U^0_{i,j}=0,\ V^0_{i,j}=0,\ \bar{T}^0_{i,j}=0,\ \bar{C}^0_{i,j}=0 \quad (18)$$
$$U^n_{0,j}=0,\ V^n_{0,j}=0,\ \bar{T}^0_{0,j}=0,\ \bar{C}^n_{0,j}=0$$
$$U^n_{i,0}=1,\ V^n_{i,0}=0,\ \bar{T}^n_{i,0}=1,\ \bar{C}^n_{i,0}=1 \quad (19)$$
$$U^n_{i,L}=0,\ V^n_{i,L}=0,\ \bar{T}^n_{i,L}=0,\ \bar{C}^n_{i,L}=0, \text{ where } L\to\infty$$

The subscripts i and j designate the grid points with X and Y coordinates respectively and the superscript n represents a value of time, $\tau = n\cdot\Delta\tau$ where $n = 0, 1, 2, \ldots$.

4. Stability and Convergence Analysis

Since an explicit procedure is being used, the analysis will remain incomplete unless the discussion of the stability and convergence of the finite difference scheme. For the constant mesh sizes the stability criteria of the scheme may be established as follows.

The eq. (14) will be ignored since $\Delta\tau$ does not appear in it. The general terms of the Fourier expansion for U, $\bar{T}$ and $\bar{C}$ at a time arbitrarily called $\tau=0$ are all $e^{i\alpha X}e^{i\beta Y}$, apart from a constant, where $i=\sqrt{-1}$. At a time τ, these terms become:

$$U : \psi(\tau)e^{i\alpha X}e^{i\beta Y}$$
$$\bar{T} : \theta(\tau)e^{i\alpha X}e^{i\beta Y} \quad (20)$$
$$\bar{C} : \phi(\tau)e^{i\alpha X}e^{i\beta Y}$$

and after the time-step these terms will become:

$$U : \psi'(\tau)e^{i\alpha X}e^{i\beta Y}$$
$$\bar{T} : \theta'(\tau)e^{i\alpha X}e^{i\beta Y} \quad (21)$$
$$\bar{C} : \phi'(\tau)e^{i\alpha X}e^{i\beta Y}.$$

Substituting (20) and (21) into Eqs. (15)-(17), regarding the coefficients U and V as constants over any one time-step, we obtain the following equations upon simplification:

$$\frac{\psi'(\tau)-\psi(\tau)}{\Delta\tau}+U\frac{\psi(\tau)\left(1-e^{-i\alpha\Delta X}\right)}{\Delta X}+V\frac{\psi(\tau)\left(e^{i\beta\Delta Y}-1\right)}{\Delta Y} = \left[\frac{1}{R_e}\left(\frac{b^2}{a^2}\right)+M\left(1-U\right)\right]e^{-i\alpha X}e^{-i\beta Y}+\frac{2\psi(\tau)\left(\cos\beta\Delta Y-1\right)}{\left(\Delta Y\right)^2} \quad (22)$$

$$\frac{\theta'(\tau)-\theta(\tau)}{\Delta\tau}+U\frac{\theta(\tau)\left(1-e^{-i\alpha\Delta X}\right)}{\Delta X}+V\frac{\theta(\tau)\left(e^{i\beta\Delta Y}-1\right)}{\Delta Y}=\left(\frac{1+R}{P_r}\right)\frac{2\theta(\tau)\left(\cos\beta\Delta Y-1\right)}{\left(\Delta Y\right)^2} +E_cU\psi(\tau)\left\{\frac{\left(e^{i\beta\Delta Y}-1\right)}{\Delta Y}\right\}^2+N_b\bar{C}\theta(\tau)\left\{\frac{\left(e^{i\beta\Delta Y}-1\right)}{\Delta Y}\right\}^2+N_t\bar{T}\theta(\tau)\left\{\frac{\left(e^{i\beta\Delta Y}-1\right)}{\Delta Y}\right\}^2 \quad (23)$$

$$\frac{\phi'(\tau)-\phi(\tau)}{\Delta\tau}+U\frac{\phi(\tau)\left(1-e^{-i\alpha\Delta X}\right)}{\Delta X}+V\frac{\phi(\tau)\left(e^{i\beta\Delta Y}-1\right)}{\Delta Y}$$
$$=\frac{1}{L_e}\left[\left\{\frac{2\phi(\tau)(\cos\beta\Delta Y-1)}{(\Delta Y)^2}\right\}+\left(\frac{N_t}{N_b}\right)\cdot\left\{\frac{2\theta(\tau)(\cos\beta\Delta Y-1)}{(\Delta Y)^2}\right\}\right] \tag{24}$$

The eq. (22), (23) and (24) can be written in the following form:

$$\psi' = A\psi \tag{25}$$
$$\theta' = B\theta + E\psi \tag{26}$$
$$\phi' = J\phi + K\theta \tag{27}$$

where

$$A=1-U\frac{\Delta\tau}{\Delta X}\left(1-e^{-i\alpha\Delta X}\right)-V\frac{\Delta\tau}{\Delta Y}\left(e^{i\beta\Delta Y}-1\right)+\frac{2\Delta\tau}{(\Delta Y)^2}(\cos\beta\Delta Y-1)+\frac{1}{R_e}\frac{1}{U}\left(\frac{b^2}{a^2}\right)\Delta\tau$$
$$+\frac{M}{U}(1-U)\Delta\tau,$$

$$B=1-U\frac{\Delta\tau}{\Delta X}\left(1-e^{-i\alpha\Delta X}\right)-V\frac{\Delta\tau}{\Delta Y}\left(e^{i\beta\Delta Y}-1\right)+\left(\frac{1+R}{P_r}\right)\frac{2(\cos\beta\Delta Y-1)}{(\Delta Y)^2}\Delta\tau$$
$$+N_b\overline{C}\left\{\frac{\left(e^{i\beta\Delta Y}-1\right)}{\Delta Y}\right\}^2\Delta\tau+N_t\overline{T}\left\{\frac{\left(e^{i\beta\Delta Y}-1\right)}{\Delta Y}\right\}^2\Delta\tau,$$

$$E=E_cU\frac{\Delta\tau}{(\Delta Y)^2}\left(e^{i\beta\Delta Y}-1\right)^2,$$

$$J=1-U\frac{\Delta\tau}{\Delta X}\left(1-e^{-i\alpha\Delta X}\right)-V\frac{\Delta\tau}{\Delta Y}\left(e^{i\beta\Delta Y}-1\right)+\frac{1}{L_e}\frac{2\Delta\tau}{(\Delta Y)^2}(\cos\beta\Delta Y-1),$$

and

$$K=\frac{1}{L_e}\left(\frac{N_t}{N_b}\right)\frac{2\Delta\tau}{(\Delta Y)^2}(\cos\beta\Delta Y-1).$$

Hence the eqs. (25), (26) and (27) can be expressed in matrix notation as:

$$\begin{bmatrix}\psi'\\ \theta'\\ \phi'\end{bmatrix}=\begin{bmatrix}A & 0 & 0\\ E & B & 0\\ 0 & K & J\end{bmatrix}\begin{bmatrix}\psi\\ \theta\\ \phi\end{bmatrix} \tag{28}$$

that is, $\eta' = T\eta$

where $\eta' = \begin{bmatrix} \psi' \\ \theta' \\ \phi' \end{bmatrix}$, $T = \begin{bmatrix} A & 0 & 0 \\ E & B & 0 \\ 0 & K & J \end{bmatrix}$ and $\eta = \begin{bmatrix} \psi \\ \theta \\ \phi \end{bmatrix}$

For obtaining the stability condition we have to find out eigenvalues of the amplification matrix T, but this study is very difficult since all the elements of T are different. Hence the problem requires that the Eckert Number E_c be assumed too small to be zero. Under this consideration we have, $E = 0$. The amplification matrix becomes:

$$T = \begin{bmatrix} A & 0 & 0 \\ 0 & B & 0 \\ 0 & K & J \end{bmatrix}$$

After simplification of the matrix T, we get the following eigenvalues:
$\lambda_1 = A$, $\lambda_2 = B$ and $\lambda_3 = J$.

For stability, each eigenvalues λ_1, λ_2 and λ_3 must not exceed unity in modulus. Hence the stability condition is
$|A| \le 1$, $|B| \le 1$ and $J \le 1$, for all α, β.

Now we assume that U is everywhere non-negative and V is everywhere non-positive. Thus

$$B = 1 - 2\left[a + b + 2c\left(\frac{1+R}{P_r} + N_b\overline{C} + N_t\overline{T}\right)\right]$$

where $a = U\dfrac{\Delta\tau}{\Delta X}$, $b = |V|\dfrac{\Delta\tau}{\Delta Y}$ and $c = \dfrac{\Delta\tau}{(\Delta Y)^2}$

The coefficients a, b and c are real and non-negative. We can demonstrate that the maximum modulus of B occurs when $\alpha\Delta X = m\pi$ and $\beta\Delta Y = n\pi$, where m and n are integers and hence B is real. The value of $|B|$ is greater when both m and n are odd integers.
To satisfy the second condition $|B| \le 1$, the most negative allowable value is $B = -1$. Therefore the first stability condition is

$$2\left[a + b + 2c\left(\frac{1+R}{P_r} + N_b\overline{C} + N_t\overline{T}\right)\right] \le 2 \tag{29}$$

i.e.,

$$U\frac{\Delta\tau}{\Delta X} + |V|\frac{\Delta\tau}{\Delta Y} + \frac{2(1+R)}{P_r}\frac{\Delta\tau}{(\Delta Y)^2} + 2N_b\overline{C}\frac{\Delta\tau}{(\Delta Y)^2} + 2N_t\overline{T}\frac{\Delta\tau}{(\Delta Y)^2} \le 1 \tag{30}$$

Likewise, the third condition $|J| \le 1$ requires that:

$$U\frac{\Delta\tau}{\Delta X}+|V|\frac{\Delta\tau}{\Delta Y}+\frac{2}{L_e}\frac{\Delta\tau}{(\Delta Y)^2}\le 1 \tag{31}$$

Therefore, the stability conditions of the method are:

$$U\frac{\Delta\tau}{\Delta X}+|V|\frac{\Delta\tau}{\Delta Y}+\frac{2(1+R)}{P_r}\frac{\Delta\tau}{(\Delta Y)^2}+2N_b\overline{C}\frac{\Delta\tau}{(\Delta Y)^2}+2N_t\overline{T}\frac{\Delta\tau}{(\Delta Y)^2}\le 1 \text{ and}$$

$$U\frac{\Delta\tau}{\Delta X}+|V|\frac{\Delta\tau}{\Delta Y}+\frac{2}{L_e}\frac{\Delta\tau}{(\Delta Y)^2}\le 1.$$

Since from the initial condition, $U=V=\overline{T}=\overline{C}=0$ at $\tau=0$ and the consideration due to stability and convergence analysis is $E_c<<1$ and $R\ge 0.5$. Hence convergence criteria of the method are $P_r\ge 0.375$ and $L_e\ge 0.25$.

5. Results and Discussion

In order to investigate the physical representation of the problem, the temperature and species concentration within the boundary layer have been computed for different values of Magnetic parameter M, Radiation parameter R, Prandtl number P_r, Eckert number E_c, Lewis number L_e, Brownian motion parameter N_b, Thermophoresis parameter N_t, Local Reynolds number R_e and velocity parameter $\frac{b}{a}$. To obtain the steady-state solutions of the computation, the calculation has been carried out up to non-dimensional time, $\tau=5$ to 80. The temperature and concentration profiles do not show any change after non-dimensional time, $\tau=40$. Therefore, the solution for $\tau\ge 40$ is steady-state solution. The graphical representation of the problem is showed in Figures 3-8.

In Figures 3-8, the dimensionless temperature and concentration distributions are plotted against Y for different non-dimensional times, $\tau=5$ to 40 and the corresponding values of M, R, P_r, E_c, L_e, N_b, N_t, R_e and $\frac{b}{a}$. The temperature distribution and the concentration distribution are plotted for different values of N_b, in Figures 3 and 4 respectively. It is observed that, the concentration profiles decrease with increase of N_b, while it is reverse for temperature profiles.

Figure 5 shows the dimensionless temperature distribution for different values of P_r, for $\tau=5, 10$ and 40; as P_r increases, the temperature decreases. Figure 6 shows the corresponding dimensionless concentration distribution for different values of L_e; the concentration profiles decrease with increase in L_e. For all the time-steps tested, as R increases the temperature gradually increases (Figure 7) and the concentration decreases as (Figure 8).

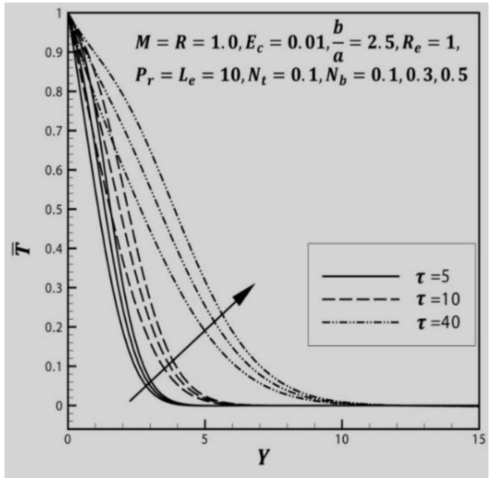

Figure 3. Temperature profiles for different values of $N_\mathbf{b}$.

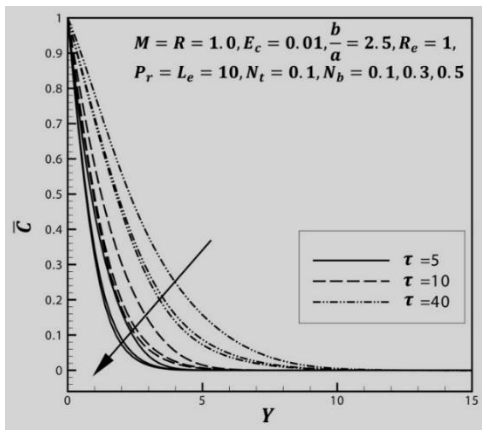

Figure 4. Concentration profiles for different values of $N_\mathbf{b}$.

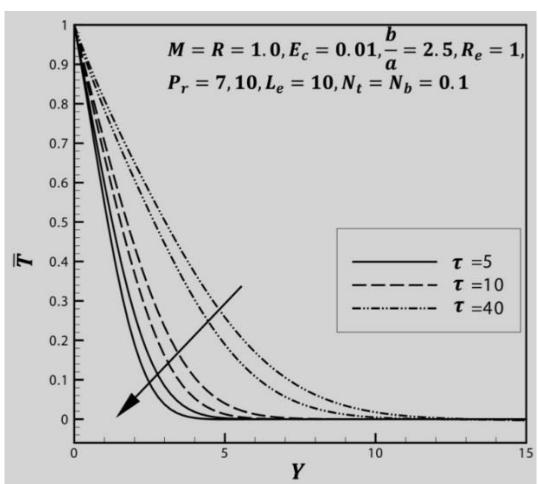

Figure 5. Temperature profiles for different values of P_r .

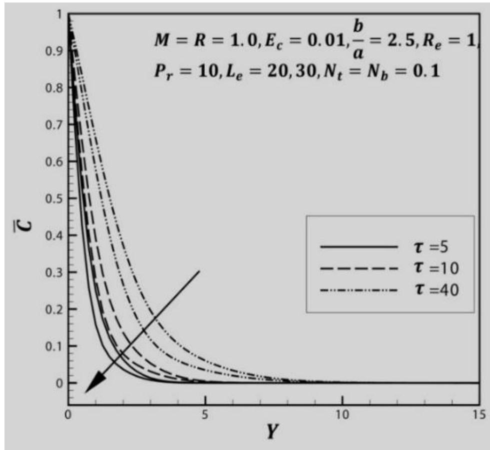

Figure 6. Concentration profiles for different values of L_e .

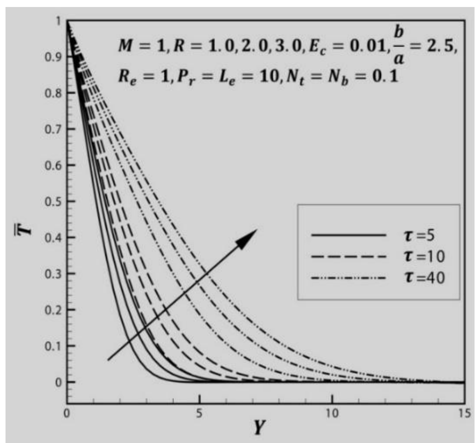

Figure 7. Temperature profiles for different values of R .

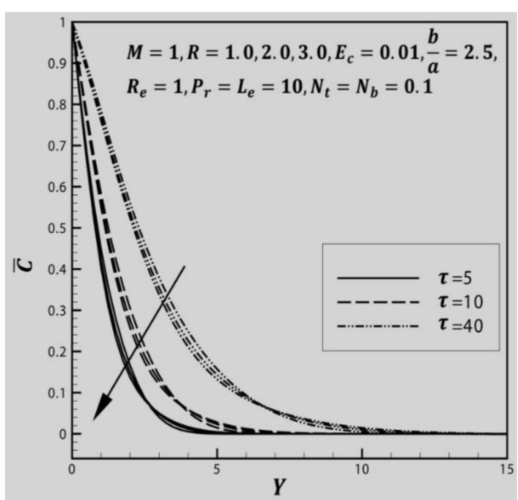

Figure 8. Concentration profiles for different values of R .

6. Conclusion

Study of unsteady MHD radiative laminar boundary layer flow of a nanofluid due to stretching sheet is presented. The explicit finite difference method with stability and convergence analysis has been employed to analyze the model. The effects of various parameters on the temperature and concentration distributions are shown graphically. The effects of thermal radiation and magnetic field on the heat and mass transfer characteristics are also studied. The following conclusions are drawn from the study:

1. For increasing the Brownian parameter, the temperature profiles are found to be increasing whereas the concentration distribution decreases. Therefore the boundary layer thickness of concentration is smaller than the thermal boundary layer thickness.
2. Thermal boundary layer thickness decreases as Prandtl number increases.
3. Concentration boundary layer thickness decreases as Lewis number increases.
4. The MHD and Radiation effect through the boundary layer for both temperature and concentration has a great impact on flow patterns. Thermal boundary layer thickness gradually increases with increase in Radiation parameter whereas the concentration boundary layer thickness decreases.

Acknowledgment

One of the authors, Md. Shakhaoath Khan, would like to acknowledge the National Science and Technology (NST) fellowship 2011 provided by the Ministry of Science and Technology, Government of People's Republic of Bangladesh for conducting this research as part of M.Sc. study.

References

Anjali Devi S P and Andrews J. (2011). Laminar boundary layer flow of a nanofluid over a flat plate, Int. J. of Appl. Math and Mech. 7 (6): 52-71

Bachok N, Ishak A, Pop I. (2010). Boundary layer flow of nanofluid over moving surface in a flowing fluid, Int. J. of Thermal Sciences 49:1663–1668.

Beg OA, Khan MS, Karim I, Alam MM, Ferdows M. (2014). Explicit Numerical study of Unsteady Hydromagnetic Mixed Convective Nanofluid flow from an Exponential Stretching sheet in Porous media, Applied Nanoscience 4(8): 943–957.

Carnahan B, Luther HA and Wilkes JO. (1969). Applied Numerical Methods, John Wiley and sons, New York.

Choi SUS. (1995). Enhancing Thermal Conductivity of Fluids With Nanoparticles, Development and Applications of Non-Newtonian Flows, DA Siginer and HP Wang, eds., ASME MD- vol. 231 and FED-vol. 66, USDOE, Washington, DC (United States), 99-105.

Ferdows M, Khan MS, Alam MM and Sun S. (2012). MHD Mixed convective boundary layer flow of a nanofluid through a porous medium due to an Exponentially Stretching sheet, Mathematical problems in Engineering 3(7): 2551-155.

Ferdows M, Khan MS, Bég OA, Alam MM, (2014). Numerical Study of Transient Magnetohydrodynamic Radiative Free Convection Nanofluid Flow from a Stretching Permeable Surface, Proceedings of the Institution of Mechanical Engineers, Part E: Journal of Process Mechanical Engineering, 228 (3):181-196.

Hamad MAA, Ferdows M. (2012). Similarity solution of boundary layer stagnation-point flow towards a heated porous stretching sheet saturated with a nanofluid with heat absorption/generation and suction/blowing: A lie group analysis, Comm. in Nonl. Sci. Num. Simul. 17: 132-140.

Hamad MAA. (2011). Analytical solution of natural convection flow of a nanofluid over a linearly stretching sheet in the presence of magnetic field, Int. Comm. In Heat and Mass Transfer 38: 487-49.

Hamad MAA, Pop I. (2011). Scaling transformations for boundary layer stagnation-point flow towards a heated permeable stretching sheet in a porous medium saturated with a nanofluid and heat absorption/generation effects , Transport in Porous Media 87: 25-39.

Hamad MAA, Pop I, Ismail AI. (2011). Magnetic field effects on free convection flow of a nanofluid past a semi-infinite vertical flat plate, Nonlinear Analysis, Real World Applications, 12: 1338–1346.

Jang SP, Choi S U S. (2007). Effects of Various Parameters on Nanofluid Thermal Conductivity, J. of Heat Transfer 129: 617-623.

Kang Ki, J YT and Choi CK (2004). Analysis of Convective Instability and Heat Transfer Characteristics of Nanofluids, Phys. Fluids 16: 2395-2401.

Khan MS, Wahiduzzaman M, Karim I, Islam MS, Alam MM. (2014).Heat Generation Effects on Unsteady Mixed Convection Flow from a Vertical Porous Plate with Induced Magnetic Field, Procedia Engineering 90: 238-244.

Khan MS, Karim I, Ali LE, Islam A. (2012). MHD Free Convection Boundary layer Unsteady Flow of a Nanofluid along a stretching sheet with thermal Radiation and Viscous Dissipation Effects, International Nano Letters 2 (24):1-9.

Khan MS, Alam MM, Ferdows M. (2013). Effects of Magnetic field on Radiative flow of a Nanofluid past a Stretching Sheet, Procedia Engineering 56: 316-322.

Khan WA, Pop I. (2010). Boundary layer flow of nanofluid past a stretching sheet, Int. J.Of Heat and Mass Transfer 53:2477-2483.

Khan WA, Pop I. (2011).Free Convection Boundary Layer Flow Past a Horizontal Flat Plate Embedded in a Porous Medium Filled with a Nanofluid, J. Heat Trans.133: 9.

Kuznetsov AV, Nield DA. (2009). The Cheng–Minkowycz Problem for Natural Convective Boundary-layer Flow in a Porous Medium Saturated by a Nanofluid, Int. J. of Heat and Mass Transfer, 52: 5792 – 5795.

Kuznetsov AV, Nield DA. (2010). Natural convective boundary-layer flow of a nanofluid past a vertical plate, International Journal of Thermal Sciences 49: 243–247.

Kumar H. (2009). Radiative Heat Transfer with Hydro magnetic flow and Viscous Dissipation over a Stretching surface in the Presence of Variable Heat Flux, Thermal Sci., 13: 163-169.

Pop I and Na TY (1996). Unsteady flow past a stretching sheet, Mechanics Research Communications 23(4): 413-422.

Rohsenow WM, Harnett JP, Cho YI. (1998). Handbook of Heat transfer, 3rd edition, McGraw-Hill, New York.

Sattar MA, Alam MM. (1994). Thermal diffusion as well as transpiration effects on MHD free convection and mass transfer flow past an accelerated vertical porous plate, Indian Journal of Pure and Applied Mathematics 25:679.

Singh P, Jangid A, Tomer NS, Sinha D. (2010). Effects of Thermal Radiation and Magnetic Field on Unsteady Stretching Permeable Sheet in Presence of Free Stream Velocity, International Journal of Information and Mathematical Sciences 6 (3): 63-69.

Takabi B, Salehi S. (2014). Augmentation of the Heat Transfer Performance of a Sinusoidal Corrugated Enclosure by Employing Hybrid Nanofluid, Advances in Mechanical Engineering 6:147059.

Takabi B, Shokouhmand H. (2015). Effects of Al2O3-Cu/water hybrid nanofluid on heat transfer and flow characteristics in turbulent regime", International Journal of Modern Physics C 26(4): 1550047.

Wahiduzzaman M, Khan MS, Karim I, Biswas P, Uddin MS. (2015).Viscous Dissipation and Radiation effects on MHD Boundary Layer Flow of a Nanofluid past a Rotating Stretching Sheet, Applied Mathematics 6: 547-567.

Wahiduzzaman M, Khan MS, Karim I. (2015).MHD convective stagnation flow of nanofluid over a shrinking surface with thermal radiation, heat generation and chemical reaction, Procedia Engineering, 105: 398-405.

Wang CY. (1984). The three-dimensional flow due to a stretching surface, Phys. Fluids, 27: 1915-1917.